

X-ray Spectroscopic Quantification of Phosphorus Transformation in Saharan Dust during Trans-Atlantic Dust Transport

Than T. N. Dam, Alon Angert, Michael D. Krom, Laura Bigio, Yongfeng Hu, Kevin A. Beyer, Olga L. Mayol-Bracero, Gilmarie Santos-Figueroa, Casimiro Pio, and Mengqiang Zhu*



Cite This: *Environ. Sci. Technol.* 2021, 55, 12694–12703



Read Online

ACCESS |

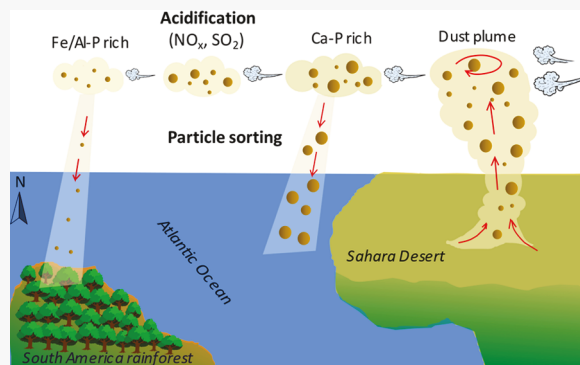
Metrics & More

Article Recommendations

Supporting Information

ABSTRACT: Saharan dust is an important phosphorus (P) supply to remote and oligotrophic parts of the oceans and American lowland tropical rainforests. Phosphorus speciation in aeolian dust ultimately controls the release and bioavailability of P after dust deposition, but the speciation in Saharan dust and its change during the trans-Atlantic transport remains unclear. Using P K-edge X-ray absorption near edge structure (XANES) spectroscopy, we showed that with increasing dust traveling distance from the Sahara Desert to Cape Verde and to Puerto Rico, about 570 and 4000 km, respectively, the proportion of Ca-bound P (Ca-P), including both apatite and nonapatite forms, decreased from 68–73% to 50–71% and to 21–37%. The changes were accompanied by increased iron/aluminum-bound P proportion from 14–25% to 23–46% and to 44–73%, correspondingly. Laboratory simulation experiments suggest that the changes in P speciation can be ascribed to increasing degrees of particle sorting and atmospheric acidification during dust transport. The presence of relatively soluble nonapatite Ca-P in the Cape Verde dust but not in the Puerto Rico dust is consistent with the higher P water solubility of the former than the latter. Our findings provide insights into the controls of atmospheric processes on P speciation, solubility, and stability in Saharan dust.

KEYWORDS: Saharan dust, phosphorus, speciation, XANES spectroscopy, trans-Atlantic dust transport



1. INTRODUCTION

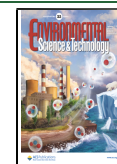
The offshore oligotrophic oceans and lowland tropical rainforests rely heavily on atmospheric deposition of long-range transported mineral dust as a major external supply of phosphorus (P).^{1,2} Mineral dust-borne P increases phytoplankton growth and (together with iron) nitrogen fixation rates in oceanic regions³ and partially sustains tropical rainforests and other ecosystems with low weathering-derived nutrient input.^{4–6} Consequently, the dust-borne P supply affects the primary productivity of terrestrial and marine ecosystems and the global carbon cycle.⁷

The Sahara Desert is the largest and most important global dust source.⁸ Annually, around 182 million tons of Saharan mineral dust are carried by the African trade winds.⁴ Approximately 28 million tons of that amount are deposited onto the Amazon basin in winter and spring, fertilizing the P-poor tropical soils⁴ while the remaining amount is deposited along its transport pathway, providing an important source of nutrients to the oligotrophic open ocean gyres and the Caribbean Sea.⁹ The dust generated from the Sahara Desert is enriched in P because some of the dust source soils overlie sedimentary phosphorite bedrock or inherit sediments from the dry lake beds containing P-rich materials.^{10,11} The fate and availability of dust-borne P in P-depleted tropical soils and

seawater are different. In tropical soils, while labile P may be more readily available to plants and microorganisms than other forms, all of the soil P, including mineral-P (e.g., apatite), is eventually released through biotic or abiotic processes.^{12,13} By contrast, in the ocean, only labile P (i.e., primarily the soluble P in alkaline seawater) is available for phytoplankton uptake, while nonlabile P drops through the euphotic zone and gets buried in sediments.¹⁴ A fraction of the labile dust-borne P compounds is formed at the source and is immediately available while the initially refractory mineral-P, such as apatite, may become partially available as a result of atmospheric acidification during dust transport.^{15,16} The solubility and fate of dust-borne P after deposition are ultimately controlled by its chemical forms or speciation. While much information has been gained about the P speciation in the Saharan dust collected within or near the Sahara Desert,^{17,18} its changes and underlying mechanisms during the long-range trans-Atlantic

Received: March 9, 2021

Published: September 10, 2021



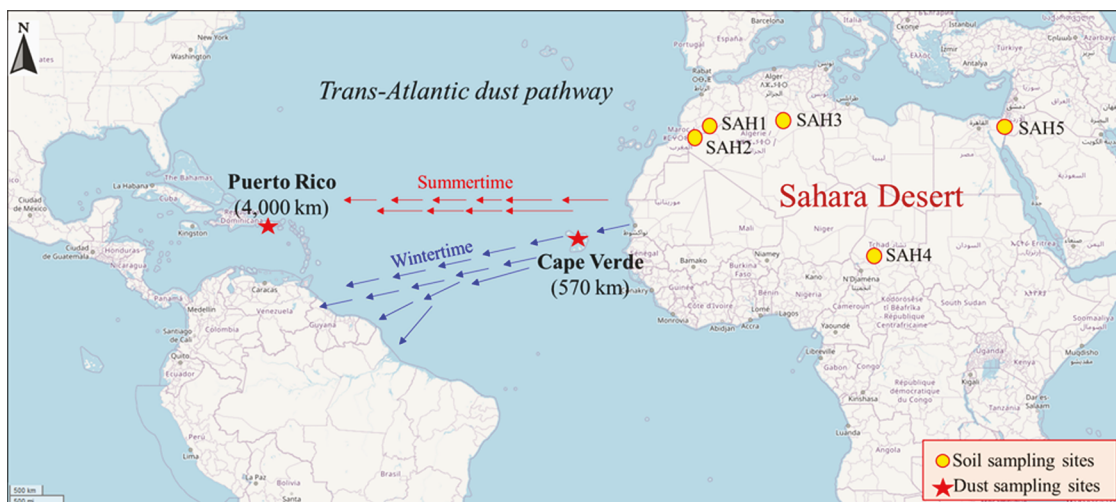


Figure 1. Dust samples were collected at Cape Verde and Puerto Rico, located ~570 and ~4000 km, respectively, downwind from the African west coast. Potential source soils were collected at different locations (SAH1–SAH5) of the Sahara Desert. The background picture is adopted from OpenStreetMap.

transport remain poorly understood. This information is critical to our understanding of the solubility, stability, and thus the bioavailability of dust-borne P. In turn, it provides insights into the effectiveness of dust inputs in supplying bioavailable P to remote and oligotrophic parts of the oceans and to the P-poor tropical rainforests of the Americas.

The speciation of P has been reported only for local and short-range transported African dusts.^{17,19} In the dust collected from the Bodélé Depression within the Sahara Desert, both calcium-bound P (Ca-P) and Fe-bound P (Fe-P) were important species,¹⁷ and the dust had a relatively low P water solubility (2–4% of the total P). In contrast, the aeolian dust collected above the Mediterranean Sea, adjacent to the north border of Africa, contained mainly Ca-P in some samples but dominantly organic P (P_{org}) and Fe- and/or Al-bound P (Fe/Al-P) in others due to the mixing of Saharan dust rich in Ca-P with European dust of anthropogenic sources to various degrees.¹⁹ The P solubility of the North African aerosols was $15.5 \pm 14.1\%$ of the total P on average, much lower than that of the European aerosols ($54.0 \pm 5.6\%$).¹⁹ Due to the short travel distances of the Saharan dust reported previously,^{17,19} their results on P speciation may not be applicable to the long-range transported dust from the Sahara Desert to the Caribbean Sea and American tropical rainforests. The trans-Atlantic dust travels across a distance of at least 4000 km. The travel takes about a week (5–6 days),^{20,21} presumably allowing for a high degree of atmospheric acidic processing, particle sorting, and physical mixing with other dust sources, which may strongly alter P speciation and solubility.²²

The P speciation in dust can be altered via interaction with acids in clouds and aerosols^{2,7,23} produced by acidic precursors from anthropogenic sources, e.g., NO_x and SO₂.²⁴ In such acidic environments, reaction with acids lowers the pH and can substantially alter the mineralogy, geochemistry, and solubility of nutrients (e.g., Fe and P) in the dust.^{16,25–27} The Saharan dust deposited in Bermuda, about 5000 km from the western edge of Africa, underwent substantial atmospheric acidification, increasing the iron solubility and contents of ferrous iron,²⁸ although minimal chemical processing was suggested by unchanged hygroscopic properties of Saharan dust deposited in Puerto Rico.²⁹ Laboratory studies simulated atmospheric

acidification using cycles of alternate pH 5 and pH 2 to represent pH conditions of clouds and aerosols, respectively.^{25–27,30} Upon acidification, both P and Fe compounds in the dust can be partially dissolved,^{16,25–27,30} increasing their solubility,²⁷ and reactive Fe minerals, such as ferrihydrite, were also produced.^{25,27} The dissolution of apatite in aeolian dust increased with increasing acidity, even before the complete consumption of carbonates by acids.¹⁶ Similarly, a portion of Ca-P in aeolian dust deposited in the Rocky Mountain region was dissolved in synthetic alpine lake water of pH 5 and some of the released P resorbed back onto Fe oxides within the dust, leading to increased Fe-P.³¹

Dust particle sorting is another potential atmospheric process to affect P speciation and solubility during dust transport. Due to different gravitational settling velocities of particles in the atmosphere, the size of dust particles decreases with increasing transport distance.^{32,33} Phosphorus speciation in dust particles varies with particle size. The P in the fine size fraction is dominated by Fe/Al-P, while the coarse fraction contains more Ca-P because Fe and Al oxides and phyllosilicates accumulate in the fine fraction.³⁴ The finer soil particles also have higher P contents and sorption capacities than the coarser ones due to larger specific surface areas and higher abundance of metal oxides.^{35,36} Moreover, mixing with other sources, including sea salt aerosols, biomass-burning particles, anthropogenic aerosols, volcanic ash, etc.^{19,37,38} during Saharan mineral dust transport can alter the dust-borne P speciation as well.

In the present study, we determined P speciation in the Saharan dust and potential dust source soils using P K-edge X-ray absorption near edge structure (XANES) spectroscopy and assessed the role of atmospheric acidification and particle sorting in altering P speciation during long-term trans-Atlantic dust transport. The dust samples were collected in different dust events at either Puerto Rico or Cape Verde Island on the east to west Atlantic transect. Although Cape Verde and Puerto Rico are not on the same dust transport pathway, they can provide insights into changes in P speciation and dust mineralogy with increasing distance from the dust source. Phosphorus speciation in bulk versus the fine fraction of the Saharan soils and the dust treated with simulated atmospheric

acidification were characterized to evaluate how particle sorting and atmospheric acidification would alter P speciation during the dust transport. Furthermore, we explored the relationship between the determined P speciation and P water solubility of the dust samples.

2. MATERIALS AND METHODS

2.1. Dust and Soil Sampling. Aeolian dust samples were collected during major Saharan dust events by active samplers equipped with a particulate matter (PM₁₀) size cutoff device in Cape Verde archipelago and in Puerto Rico, operating with a flow rate of 1.13 m³ min⁻¹.^{18,39} Twelve and six dust samples were collected in Cape Verde and Puerto Rico, respectively, and used in the present study. The specific sampling dates, sampler, and filter types are listed in Table S1. Both sampling sites were on the trans-Atlantic Saharan dust transport pathway, located ~570 and ~4000 km away from the west coast of Africa, respectively (Figure 1). In Cape Verde, dust samples were collected using a high-volume air sampler at the former airport of Praia (14.92°N, 23.48°W; altitude 98 m). In Puerto Rico, five dust samples (PR1–PR5) were collected using a high-volume air sampler in the nature reserve of Cabezas de San Juan (18.38107°N 65.61775°W, altitude 67 m), specifically in the Cape San Juan Atmospheric Observatory at the northeastern tip of the island. This site had a good exposure to the easterly trade winds, which transport Saharan dust. The sample PR6 was collected using stacked-filter units at the University of Puerto Rico in San Juan during a Saharan dust incursion. The Cape Verde dust samples were collected during the winter of 2011 and the Puerto Rico dust samples in the summer of 2015. The different dust collection seasons at the two locations were due to the fact that the Saharan dust reaches Cape Verde only during winter and Puerto Rico only during summer.^{38,40} The two locations, together with the Sahara Desert, form a long-range dust transport pathway although the dust samples were not produced from the same dust plumes and events. After collection, the filters loaded with dust were air-dried prior to all of the analyses. The collection of the dust samples during major Saharan dust events was to minimize potential contributions from local dust sources. The origin of the dust samples from the Sahara Desert was confirmed by satellite observation and back-trajectory analyses in previous studies.^{18,39} More details about the dust collection and other dust characteristics, including total elemental composition, were reported in those studies as well.^{18,39}

In addition to the dust samples, surface soil samples (top 1 cm) were collected at various locations from four out of six major trans-Atlantic Saharan dust source areas in the Sahara Desert (SAH1–SAH4) (Figure 1).⁴¹ Also, a dust sample that had traveled a relatively short distance away from northern Africa was collected in Jerusalem, Israel (SAHS). This dust sample was regarded as a soil sample, given the fact that its properties were similar to those of the northern Saharan surface soils.⁴¹ Other potential dust source areas in the Sahara Desert were difficult to access due to logistic challenges. The details about the soil collection are provided elsewhere¹⁸ with the sampling locations in Table S2.

2.2. Fine Soil Fraction Separation. Phosphorus speciation in the fine soil fractions versus the bulk soil was determined to evaluate the particle sorting effect on P speciation. The fine soil fraction (<10 μm) was separated using the pipette method.⁴² Specifically, 0.2 g of each soil was mixed with deionized (DI) water of pH 6.5 in a 50-mL

volumetric flask. The suspension was settled for 20 min when the top 10 cm depth of the suspension was transferred to a clean tube. The suspension was filtered through a 0.2-μm P-free membrane filter, and the particles collected on the filter were air-dried for P K-edge XANES analyses. The P concentration in the solution was measured by the molybdate blue method using a UV-vis spectrophotometer (UV-1600PC, VWR) at a wavelength of 882 nm to estimate the soluble P loss to the solution during the size separation.⁴³

2.3. X-ray Diffraction (XRD) and Scanning Electron Microscopy (SEM). All soil (both bulk and fine fraction) and dust samples were characterized using synchrotron-based XRD (SR-XRD) at beamlines 17-BM-B or 11-ID-B using X-rays of 0.4359 or 0.2125 Å at the Advanced Photon Source, Argonne National Laboratory, to identify mineral phase changes during dust transport. The diffraction data were background removed and converted to 2θ with Cu Kα radiation ($\lambda = 1.5406$ Å) for phase identification using MDI Jade 6.0 (Livermore, CA). Changes in sizes and morphology of dust particles were characterized using SEM. The SEM images could also indicate whether biomass-burning particles were present in the dust samples.³⁸ Details on SR-XRD and SEM characterization techniques are provided in Text S1.

2.4. Atmospheric Acidification Processing Simulation. The acidification experiments were performed on two selected Cape Verde dust samples (CV098 and CV135) to evaluate P speciation changes during atmospheric acidification, following a protocol used in previous studies.^{25–27,30} Due to the short traveling distance, the Cape Verde dust represented the Saharan dust during the early stage of the transport. The simulation was conducted in 10 days, including 10 continuous cycles, and each cycle consisted of two 12 h incubations at pH 5 and pH 2, respectively, representing cloud droplet and aerosol conditions.^{25,27} Five pieces of dust-loaded quartz membrane filters (each piece was cut in a round shape of 1/4 in. in diameter) of CV098 or CV135 were transferred to 1 L of pH 5 deionized (DI) water. The solution was continuously stirred on a stirrer plate at a slow speed (150 round min⁻¹). The solution pH, measured by a pH meter, was maintained at the target pH by adding either H₂SO₄ or NH₄OH during each incubation. Solid residues and solution samples were collected only at pH 5 after 1.5, 3.5, 5.5, and 10 pH cycles. More details in the setup of the simulation experiments are provided in Text S2 and Figure S1. The treated dust membranes were then air-dried and used for the XANES analysis. Another similar experiment with dust sample CV098 was conducted by incubating the dust at pH 5 or 2 for 12 h to examine the impact of pH on the residual P speciation. The concentration of dissolved P was measured using inductively coupled plasma mass spectrometry (iCAP RQ ICP-MS, Thermo Scientific).

2.5. Phosphorus K-Edge XANES Spectroscopy. XANES spectroscopy was used to determine P speciation in all source soils, fine fractions of the source soils, and Puerto Rico dust samples, while 6 out of 12 Cape Verde dust samples were chosen for the measurement due to a limited amount of beamtime. With a linear combination fitting (LCF) analysis, XANES spectroscopy was used to identify and quantify solid P species of three main categories, Ca-P, Fe/Al-P, and organic P (P_{org}).^{31,44,45} The spectra were collected at Soft X-ray Microcharacterization Beamline, Canadian Light Source, Saskatoon, Canada. The peak maximum of the first derivative spectrum of AlPO₄ (berlinite) was set at 2152.9 eV to calibrate the beamline energy. The spectra were recorded between 2110

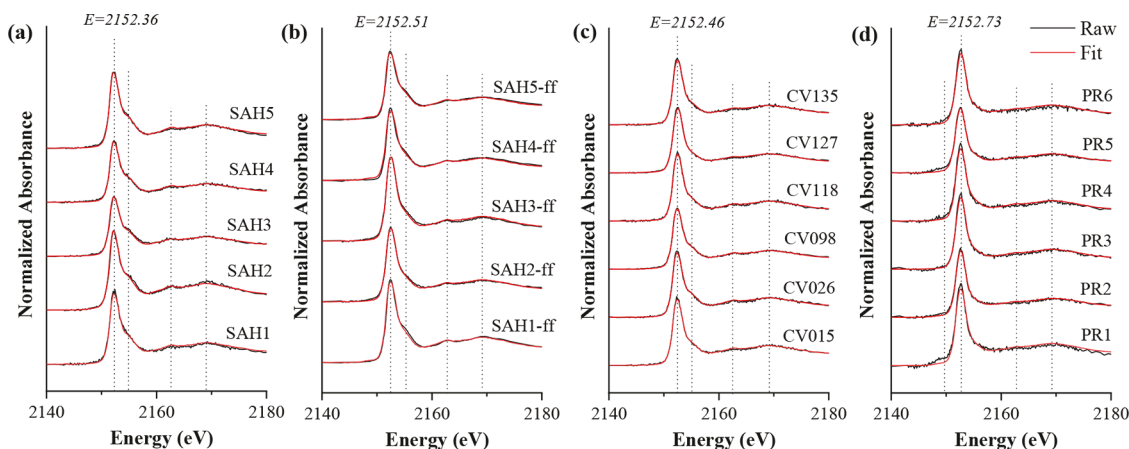


Figure 2. Phosphorus K-edge XANES spectra and their linear combination fits for (a) Saharan bulk soils, (b) Saharan fine soil fractions, (c) Cape Verde dust, and (d) Puerto Rico dust. The vertical lines indicate the white line position and spectral features to assist in the visual identification of the differences among samples.

and 2210 eV with a step size of 2 eV in the pre-edge range (2110–2140 eV), 0.15 eV at the edge (2140–2175 eV), and 0.75 eV in the post-edge region (2175–2210 eV). All samples were scanned twice and averaged to improve the signal-to-noise ratio. To determine P speciation, the XANES spectra were background removed and normalized prior to the LCF analysis with a pool of P reference spectra. The set of references included well-crystallized hydroxyapatite and poorly crystalline apatite as well as $\text{Ca}(\text{H}_2\text{PO}_4)_2\cdot\text{H}_2\text{O}$, representing two major groups of Ca-P species (i.e., apatite Ca-P and nonapatite Ca-P) of different solubility; a combination of PO_4^{3-} adsorbed kaolinite or amorphous Al hydroxide at pH 5.5 to represent Al-P; a combination of PO_4^{3-} adsorbed on goethite at pH 5 and amorphous FePO_4 to represent Fe-P; and sodium phytate, β -glycerophosphate disodium hydrate, and sodium phytate adsorbed on ferrihydrite, together representing P_{org} . The standards with high P concentrations were measured in the total electron yield mode to avoid self-absorption. Our previous studies showed that the reference pool can well represent major P species present in aeolian dust and dryland soils.^{31,45} In the present study, $\text{Ca}(\text{H}_2\text{PO}_4)_2\cdot\text{H}_2\text{O}$ was used to represent nonapatite Ca-P species to determine how the Ca-P pool in the dust was altered with respect to apatite. The nonapatite Ca-P is supposed to have a higher solubility and be more readily available compared to apatite Ca-P. While the XANES-LCF analysis generally has a considerable amount of uncertainty in differentiating individual Ca-P species, the spectra of $\text{Ca}(\text{H}_2\text{PO}_4)_2\cdot\text{H}_2\text{O}$ and apatite differed greatly from each other (Figure S2). As a rule of thumb, the detection limit of the LCF analysis is $\sim 10\%$. More details on the XANES data collection and analyses are provided in Text S3.

2.6. Determination of Organic P Contributions. The proportions of P_{org} in both Puerto Rico and Cape Verde dust samples were also determined using the ashing method,⁴⁶ which were compared to the XANES results that can have relatively large uncertainties in quantifying P_{org} . Details on the measurement are presented in Text S4. Unfortunately, there were not enough materials remaining from the six Cape Verde dust samples after the XANES analysis; so, the chemical extraction was performed on the other six Cape Verde dust samples collected at the same location during the same time periods (Table S1). The two sets of Cape Verde samples presumably had similar P speciation and concentration.

3. RESULTS AND DISCUSSION

3.1. Mineralogy and Morphology of the Dust and Soil Samples.

Substantial differences were observed in the mineral composition and morphology among the dust samples and the potential dust source soils. The SR-XRD data show that the major mineral phases in the bulk source soils were quartz, calcite, and dolomite, with a small amount of kaolinite and muscovite (Figure S3a), consistent with the findings of Formenti et al.⁴⁷ These mineral phases were also present in the fine fraction soils ($<10\text{ }\mu\text{m}$, Figure S3b) and the Cape Verde dust (Figure S3c), although their relative proportions were different between the two sets of samples. The fine fraction of neither SAH2 nor SAH3 soils had enough materials to collect good quality XRD data. Minor amounts of halite (NaCl) were detected in the Cape Verde dust, suggesting the mixing of the Saharan dust with sea salt aerosols during dust transport and collection (Figure S3c). In contrast, halite was the dominant mineral in the Puerto Rico dust samples, and small amounts of quartz were also detected (Figure S3d). More importantly, no carbonates were detected by XRD (with $\sim 0.5\%$ detection limit) in the Puerto Rico dust (Figure S3d). The presence of halite in the dust samples but not in the soils and its increase from Cape Verde to Puerto Rico dust indicated an increased contribution of sea salt aerosols during dust transport.^{29,48,49} The decreased quartz content from the Cape Verde dust to the Puerto Rico dust can be ascribed to particle sorting due to the large particle size and high density of quartz,^{50,51} while both particle sorting and atmospheric acidification that dissolves carbonates could contribute to the decline of carbonates.⁵¹

The shape and size of the dust particles differ greatly between the Cape Verde and Puerto Rico dust samples and between the dust and the fine fractions of the source soils as well (Figures S4 and S5). The fine soil fractions and the Cape Verde dust contained mainly sharp-edged aggregates with a large range of particle sizes, whereas the Puerto Rico dust was dominated by smaller size and size ranges of aggregates with a more rounded shape (Figure S5), consistent with the particle sorting effects.⁵² Dissolution of calcite by acidic gases during the dust transport may also contribute to the genesis of the spherical particles.⁵³

The Saharan soil sample (SAH4) from Bodélé depression contained abundant diatoms, consistent with its origin from

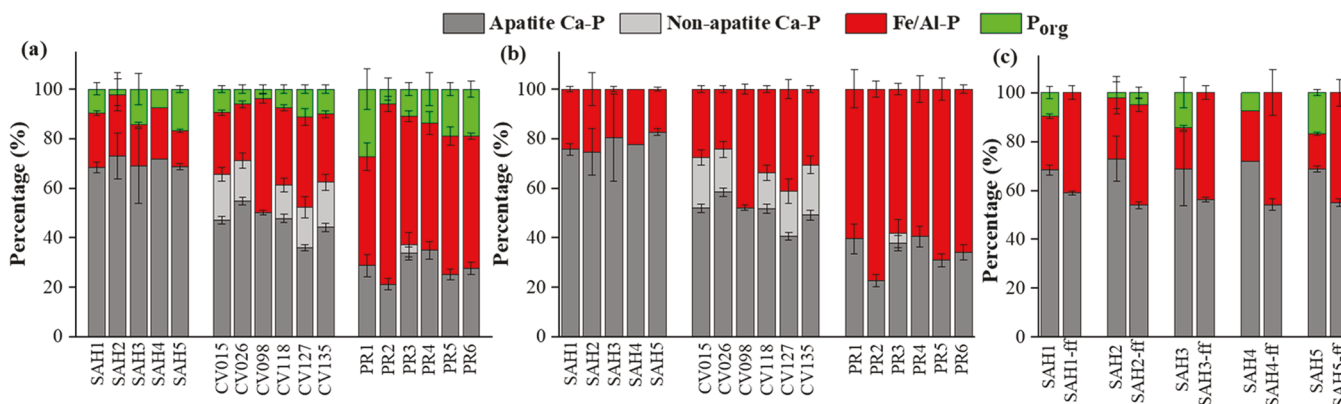


Figure 3. XANES-derived relative proportion of each P species over the total P (a) and the inorganic P pool (b). A comparison between bulk and fine fractions of Saharan soils (c). Fe/Al-P is the sum of Fe-P and Al-P. The standard deviations of the data are derived from the LCF analysis. "ff" refers to the fine soil fraction ($<10\ \mu\text{m}$).

paleolake sediments (Figure S4). However, diatoms were not observed in any dust samples, suggesting that either the dust from the Bodéle depression did not contribute greatly to the dust samples used in our study, or there was a preferential loss of diatom frustules due to their different size, shape, and/or density. Our results are consistent with the PO_4^{4-} - ^{18}O isotopic evidence from Gross et al.¹⁰ and satellite observation in Yu et al.⁵⁴ but disagree with those in Koren et al.,⁵⁵ which suggested the dominant role of Bodéle depression for dust supply to the Amazon basin.

Biomass burning can be another important source of atmospheric particles in addition to surface desert soils. Phosphorus in biomass-burning aerosols is often highly soluble and has been found to be a major fraction within some Saharan dust events.^{1,2,22} For example, a recent study showed a considerable proportion of biomass-burning materials present in the atmospheric particles sampled during Saharan dust storms transported from Africa to the Amazon Basin and Tropical Atlantic Ocean during spring.³⁸ However, only a small amount of biomass-burning particles characterized by their porous structure were observed in two of the 12 dust samples examined in the present study (CV135 and PR5, Figure S5). The result indicated that biomass burning was not an important source of particulate-P in our dust samples. The discrepancy in composition between the Puerto Rico dust in the present study and the dust studied by Barkley et al.³⁸ is probably caused more by temporal variations in the intensity of the wildfires in Africa than sampling locations.

3.2. Phosphorus Speciation. Phosphorus speciation changed substantially from the bulk dust source soils to the Cape Verde dust and to the Puerto Rico dust. The bulk and the fine fraction of the soils and Cape Verde dust all exhibited a strong shoulder peak at 2155 eV and two post-edge features at 2164 and 2169 eV in their P K-edge XANES spectra (Figure 2a–c), indicating the dominance of Ca-P species. The dominance of Ca-P reflects the alkaline condition of the dust generated from desert soils.⁵⁶ Compared to the fine fractions of the soils and the Cape Verde dust, the Puerto Rico dust had much weaker Ca-P spectral features, indicating less Ca-P and more Fe/Al-P in the Puerto Rico dust (Figure 3c). From the bulk soils to the Cape Verde dust and then to the Puerto Rico dust, in the same order of increasing dust traveling distance, the Ca-P proportion (apatite + nonapatite Ca-P) decreased from 68–73% to 50–71% and to 21–37%, while the Fe/Al-P proportion increased from 14–25% to 23–46% and then to

44–73% (Figure 3a). A similar trend was observed for the proportions of Ca-P and Fe/Al-P over total inorganic P (i.e., excluding the P_{org} contributions, as shown in Figure 3b).

Nonapatite Ca-P, represented by $\text{Ca}(\text{H}_2\text{PO}_4)_2 \cdot \text{H}_2\text{O}$ in the XANES-LCF analysis, was detected primarily in the Cape Verde dust, up to 18% (Figure 3a). Various Ca-P species could be present in the dust, and it is challenging to differentiate them using P K-edge XANES spectroscopy. However, the presence of nonapatite Ca-P in the Cape Verde dust but not in the source soils suggests that part of the apatite is transformed to Ca phosphate minerals of low Ca/P ratios or phosphate adsorbed onto Ca-bearing mineral surfaces (e.g., calcite) during the relatively short-distance transport from Sahara to Cape Verde. However, both nonapatite and apatite Ca-P fractions of the Puerto Rico dust are lower than those of the Cape Verde dust, suggesting that the Ca-P species was lost or transformed to Fe/Al-P en route to Puerto Rico.

The XANES analysis detects organic P in the soil and dust samples with the proportion ranging from 2 to 17% in the source soils, 4 to 11% in the Cape Verde dust, and 6 to 27% in the Puerto Rico dust (Figure 3a). The organic P concentrations measured by chemical extraction (Table S3) are within the 10% uncertainty of the XANES-LCF analysis, indicating that our XANES results are reliable. The higher P_{org} concentration of the Puerto Rico dust than that of the Cape Verde dust suggests a higher degree of physical mixing with P_{org}-rich aerosols of other natural or anthropogenic sources during dust transport and deposition. However, the contributions of those sources to P_{org} in the Puerto Rico dust are lower than those in the dust collected above the Mediterranean Sea¹⁸ and Panama during drying season, which had much higher P_{org} concentration.³⁵ High organic P concentrations were also observed in the aerosols that were collected at mountainous sites and had a high contribution of biogenic P.⁵⁷

The Cape Verde dust samples were collected in winter but the Puerto Rico dust in summer, which could potentially have contributed to the observed difference in P speciation. During summer, Saharan dust mainly originates from the northwest and central-west parts of the Sahara Desert, while in winter, dust source areas tend to be from the border of the Sahel activated by Harmattan winds.^{58–61} However, neither the bulk nor the fine fractions of the dust source soils collected from different regions showed substantial systematic differences in P speciation. Thus, dust collection in different seasons was unlikely to be the major reason for the different P speciation.

Mixture with other dust sources during Saharan dust transport may also affect the P speciation. However, volcanic activity and marine aerosols were reported to account for <10% of total dust-borne P.^{62,63} Our SEM results showed that biomass burning was not an important dust source. The dominant processes leading to the observed changes in the P speciation during dust transport are likely particle sorting and atmospheric acidification, as discussed below.

3.3. Effects of Particle Sorting on P Speciation. To evaluate particle sorting effects on P speciation, the P speciation of the bulk and fine fractions of the Saharan source soils were compared. The actual sizes of the separated fine soil particles were confirmed with SEM to be smaller than 10 μm (Figure S4), except for soil sample SAH4. The fine fraction of SAH4 had some larger particles of diatoms (10–15 μm) that probably had a lower density than soil particles of similar sizes and did not settle down efficiently during the size separation using the pipette method (Figure S4). The P K-edge XANES spectra of the fine fraction soils had a weaker shoulder peak and less pronounced post-edge features than the spectra of the bulk soils, suggesting less Ca-P and more Fe/Al-P in the fine fractions (Figure S2). Consistently, Ca-P accounted for 68–73% of total P in the bulk soil but only 54–59% in the fine fractions (Figure 3c and Table S4). Low P_{org} in the fine soils is consistent with that of Liu et al.,³⁴ showing that soil colloids (<1 μm soil fraction) contain much less P_{org} than bulk soils. Note that the size separation process resulted in minimal P dissolution (0.04–0.38%) (Figure S6) and thus was not expected to much affect the P speciation in the fine soil fraction. The observed effects of particle sorting on P speciation suggest that a longer dust transport distance can lead to decreased Ca-P and increased Fe/Al-P proportions in the dust because dust particles are increasingly smaller, while larger particles rich in Ca-P are lost during the transport. Nonapatite Ca-P can be associated with coarse particles and preferentially lost because it may be adsorbed on pedogenic carbonate minerals that form coatings around coarse primary particles.⁶⁴ Thus, particle sorting can contribute to the observed difference in P speciation between the Cape Verde and Puerto Rico dust.

3.4. Effects of Atmospheric Acidification on P Speciation. Atmospheric acidification can further affect P speciation in the dust.^{15,16} The solid residues were collected from the simulated acidification experiments after 1.5, 3.5, 5.5, and 10 pH cycles to examine the change of P speciation during the acidification of the two Cape Verde dust samples (CV098 and CV135). After 1.5 pH cycles, the strong Ca-P spectral features in the initial sample diminished, and the spectra were dominated by the Fe/Al-P features (Figures 4b and S7b). Specifically, the apatite-P percentage in CV098 and CV135 decreased from 50 and 44% to around 10%, while Fe/Al-P increased to 92 and 84% of the total P, respectively (Figures 4c and S7c). Nonapatite Ca-P in the dust sample (CV135) disappeared after the acidification treatment, indicating that it was dissolved and released into the solution (Figures 4c and S8). The concentration of dissolved P increased with increasing time of acidification but remained low (Figure S8) due to the high solution to solid ratio and potential re-adsorption of solubilized P back to Fe/Al minerals in the dust.³¹ In addition, a high degree of acidification of the Puerto Rico dust may partially dissolve and convert crystalline Fe and Al-bearing minerals (oxides and phyllosilicates) into poorly crystalline ferrihydrite and dissolved Fe(III) and its aluminum

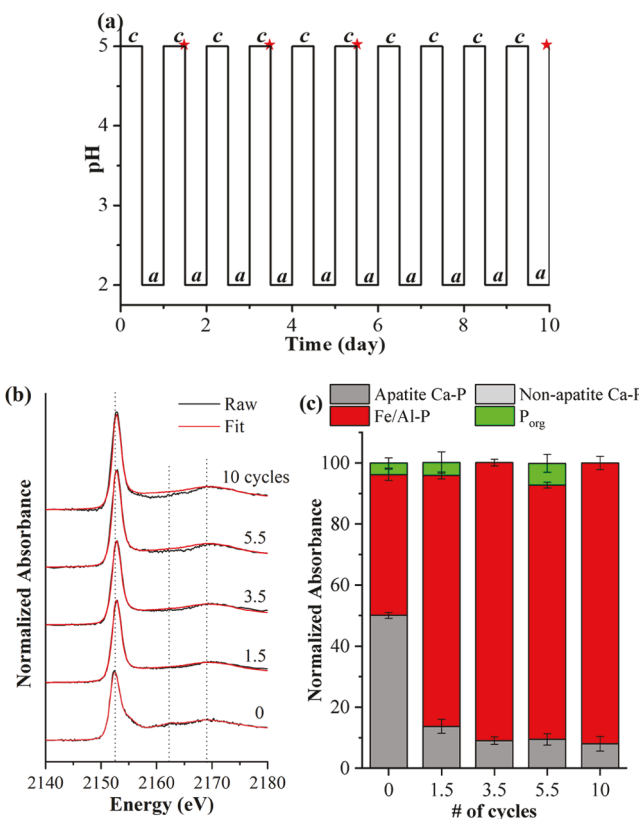


Figure 4. pH cycle of the simulated atmospheric acidification experiments under laboratory conditions (a), in which “a” refers to “aerosol condition,” “c” to “cloud droplet condition,” and red stars indicate when the solid samples were collected. Note that in the last pH cycle, the pH was adjusted to 5 before the dust residue collection. Phosphorus K-edge XANES spectra of the dust sample CV098 before and after acidification (b) and its XANES-derived P speciation (c).

equivalents,²⁵ which are very reactive and strongly adsorb P.^{28,65,66} Phosphate may also form Fe(III) or Al(III) phosphate precipitates with the reactive Fe(III) and Al(III), as identified by Fe K-edge XANES spectroscopy in the Saharan dust deposited to Bermuda, which has a similar distance to Africa as Puerto Rico.²⁸ The fact that apatite is still present in the Puerto Rico dust, accounting for 21%–34% of the total P pool after potentially strong acidification, can be due to a lack of thorough internal mixing of dust particles in clouds and aerosols.¹⁶ Alternatively, the dust experienced weak atmospheric acidification before arriving in Puerto Rico, as discussed below. Due to the shorter traveling distance, the Cape Verde dust may experience limited acidification, which, however, can be strong enough to convert some apatite to non-apatite Ca-P.

While the simulated acidification experiments suggest that atmospheric acidification can strongly affect P speciation in the dust, the simulation may overestimate the degree of the alteration occurring during dust transport. That atmospheric acidification, if it occurred, had not dissolved all apatite is in contrast to the negligible amount of Ca-P remaining after the acidification treatment with the alternate pH 2 and pH 5 treatment (Figure 4). The strong decrease of Ca-P in the acidification experiments was caused mainly by the use of pH 2 solution, as indicated by the fact that the acidification of CV098 for 12 h at pH 5 decreased the Ca-P proportion from 50 to 37% but to 7% at pH 2 (Figure S9). Thus, a weaker acidic solution (e.g., pH 5) than pH 2 may need to be used to

simulate acidification under laboratory conditions. In fact, Stockdale et al.¹⁶ used a series of increasingly acidic solutions but with their H⁺ ion activity less than that of pH 2 solution to simulate atmospheric acidification of dust, and found that more P was released from dust with increasing H⁺ ion activity until the acid-reactive P-bearing mineral pool in the dust was depleted.

3.5. Linking P Speciation to Solubility. The P solubility of the dust samples used in the present study was measured by extraction with doubly deionized water plus anion exchange resin membranes as in our previous studies.^{18,39} The Cape Verde dust samples (0.4–2.3 mg P g⁻¹ dust) had much higher P solubility than not only the source soils (0.003–0.11 mg P g⁻¹ soil) but also the Puerto Rico dust (0.08 ± 0.02 mg P g⁻¹ dust).^{10,18,39} The high P solubility of the Cape Verde dust is consistent with the presence of significant non-apatite Ca-P, which is presumably more soluble than apatite but is negligible in the source soils and the Puerto Rico dust. Our results are in contrast to the previous report in which long-range transported dust is supposed to have higher P solubility than the short-range transported dust due to increased acidification, as demonstrated in Baker et al.,²² despite NaHCO₃ solution (pH 7.2) being used for the extraction. It is likely that the non-apatite Ca-P compounds in our Cape Verde dust samples produced by limited acidification in the early transport stage were lost later through particle sorting during the transport en route to Puerto Rico. That is, atmospheric acidification may couple with particle sorting to affect P solubility in the dust. Another potential reason for the high P solubility of the Cape Verde dust is that the dust may contain particles derived from anthropogenic sources that have much higher P solubility than the dust of desert-type events.⁶⁷

4. ENVIRONMENTAL IMPLICATIONS

Phosphorus speciation in aeolian dust ultimately controls P solubility and its fate after the deposition of the dust. Our study has characterized the changes of dust-borne P speciation during a long-range dust transport across the Atlantic Ocean using XANES spectroscopy. With increasing dust traveling distance, more Fe/Al-P and less Ca-P are present in the dust, likely due to the increasing degree of particle sorting and atmospheric acidification. Despite the long-range transport, some Puerto Rico dust still contained considerable amounts of apatite-P (~30%) that is essentially not bioavailable in the euphotic zone of the oligotrophic Caribbean Sea. On the other hand, the abundant Fe/Al-P in the dust is unstable, and some of them could release into the alkaline seawater or be solubilized by marine phytoplankton. While terrestrial plants can absorb P of different forms with various strategies,^{13,68} the P composition in the dust affects the ease and rate of the P uptake by plants in the tropical rainforests. The apatite in the dust received by the ecosystem may readily dissolve and become available to plants and microorganisms in the acidic tropical rainforest soils (pH 4.2–4.9),^{69,70} although the dissolution may take a while. In fact, a recent study discovered apatite grains, some of which were likely derived from African dust, in acidic, highly weathered Hawaiian soils.⁷¹ Further research is warranted on the potential coupling between atmospheric acidification and particle sorting to affect the speciation and the solubility of dust-borne P.

■ ASSOCIATED CONTENT

SI Supporting Information

The Supporting Information is available free of charge at <https://pubs.acs.org/doi/10.1021/acs.est.1c01573>.

Details of SR-XRD, SEM, and XANES measurements; the dust sampling time and Saharan soil sites; XANES spectra of acidified dust samples; XRD patterns of all samples; SEM images of dust and fine soil fractions (PDF)

■ AUTHOR INFORMATION

Corresponding Author

Mengqiang Zhu – Department of Ecosystem Science and Management, University of Wyoming, Laramie, Wyoming 82071, United States;  orcid.org/0000-0003-1739-1055; Email: mzhu6@uwyo.edu

Authors

Than T. N. Dam – Department of Ecosystem Science and Management, University of Wyoming, Laramie, Wyoming 82071, United States;  orcid.org/0000-0002-4611-3997

Alon Angert – Institute of Earth Sciences, Hebrew University of Jerusalem, Jerusalem 9190401, Israel

Michael D. Krom – Morris Kahn Marine Research Station, Department of Marine Biology, Leon H. Charney School of Marine Science, University of Haifa, Haifa 3498838, Israel; School of Earth and Environment, University of Leeds, Leeds LS2 9JT, United Kingdom;  orcid.org/0000-0003-3386-9215

Laura Bigio – Institute of Earth Sciences, Hebrew University of Jerusalem, Jerusalem 9190401, Israel;  orcid.org/0000-0002-7154-2523

Yongfeng Hu – Canadian Light Source Inc., University of Saskatchewan, Saskatoon, Saskatchewan S7N 2V3, Canada;  orcid.org/0000-0002-7510-9444

Kevin A. Beyer – X-ray Science Division, Advanced Photon Source, Argonne National Laboratory, Lemont, Illinois 60439, United States

Olga L. Mayol-Bracero – Department of Environmental Science, University of Puerto Rico, Rio Piedras 00925, Puerto Rico

Gilmarie Santos-Figueroa – Department of Environmental Science, University of Puerto Rico, Rio Piedras 00925, Puerto Rico

Casimiro Pio – The Centre for Environmental and Marine Studies, University of Aveiro, 3810-193 Aveiro, Portugal

Complete contact information is available at: <https://pubs.acs.org/10.1021/acs.est.1c01573>

Notes

The authors declare no competing financial interest.

■ ACKNOWLEDGMENTS

This work was supported by the U.S. National Science Foundation Faculty Early Career Development Program (EAR-1752903). Dust and soil samples were collected during research projects funded by GIF Grant 1139/2011 and ISF Grant 870/08. O.L.M.-B and G.S.-F. thank the support of NSF AGS 0936879 and EAR-072247, the Conservation Trust of Puerto Rico for their use of their facilities at the nature reserve of Cabezas de San Juan, and the RISE program. A part of the research described in this work was performed at the Canadian

Light Source, which is supported by the Natural Sciences and Engineering Research Council of Canada, the National Research Council Canada, the Canadian Institutes of Health Research, the Province of Saskatchewan, Western Economic Diversification Canada, and the University of Saskatchewan. This research used resources of the Advanced Photon Source, a U.S. Department of Energy (DOE) Office of Science User Facility operated for the DOE Office of Science by Argonne National Laboratory under Contract No. DE-AC02-06CH11357.

■ REFERENCES

(1) Mahowald, N.; Jickells, T. D.; Baker, A. R.; Artaxo, P.; Benitez-Nelson, C.; Bergametti, G.; Bond, T. C.; Chen, Y.; Cohen, D.; Herut, B.; Kubilay, N.; Losno, R.; et al. Global distribution of atmospheric phosphorus sources, concentrations and deposition rates, and anthropogenic impacts. *Global Biogeochem. Cycles* **2008**, *22*, 1–19.

(2) Myriokefalitakis, S.; Nenes, A.; Baker, A. R.; Mihalopoulos, N.; Kanakidou, M. Bioavailable atmospheric phosphorus supply to the global ocean: a 3-D global modeling study. *Biogeosciences* **2016**, *13*, 6519–6543.

(3) Mills, M. M.; Ridame, C.; Davey, M.; La Roche, J.; Geider, R. J. Iron and phosphorus co-limit nitrogen fixation in the eastern tropical North Atlantic. *Nature* **2004**, *429*, 292–294.

(4) Yu, H.; Chin, M.; Yuan, T.; Bian, H.; Remer, L. A.; Prospero, J. M.; Omar, A.; Winker, D.; Yang, Y.; Zhang, Y.; Zhang, Z.; Zhao, C. The fertilizing role of African dust in the Amazon rainforest: A first multiyear assessment based on data from Cloud-Aerosol Lidar and Infrared Pathfinder Satellite Observations. *Geophys. Res. Lett.* **2015**, *42*, 1984–1991.

(5) Aciego, S. M.; Riebe, C. S.; Hart, S. C.; Blakowski, M. A.; Carey, C. J.; Aarons, S. M.; Dove, N. C.; Botthoff, J. K.; Sims, K. W. W.; Aronson, E. L. Dust outpaces bedrock in nutrient supply to montane forest ecosystems. *Nat. Commun.* **2017**, *8*, No. 14800.

(6) Chadwick, O. A.; Derry, L. A.; Vitousek, P. M.; Huebert, B. J.; Hedin, L. O. Changing sources of nutrients during four million years of ecosystem development. *Nature* **1999**, *397*, 491–497.

(7) Herbert, R. J.; Krom, M. D.; Carslaw, K. S.; Stockdale, A.; Mortimer, R. J. G.; Benning, L. G.; Pringle, K.; Browse, J. The effect of atmospheric acid processing on the global deposition of bioavailable phosphorus from dust. *Global Biogeochem. Cycles* **2018**, *32*, 1367–1385.

(8) Engelstaedter, S.; Tegen, I.; Washington, R. North African dust emissions and transport. *Earth-Sci. Rev.* **2006**, *79*, 73–100.

(9) van der Does, M.; Brummer, G.-J. A.; van Crimpen, F. C. J.; Korte, L. F.; Mahowald, N. M.; Merkel, U.; Yu, H.; Zuidema, P.; Stuut, J.-B. W. Tropical rains controlling deposition of Saharan dust across the North Atlantic Ocean. *Geophys. Res. Lett.* **2020**, *47*, No. e2019GL086867.

(10) Gross, A.; Palchan, D.; Krom, M. D.; Angert, A. Elemental and isotopic composition of surface soils from key Saharan dust sources. *Chem. Geol.* **2016**, *442*, 54–61.

(11) Yang, X.; Post, W. M.; Thornton, P. E.; Jain, A. The distribution of soil phosphorus for global biogeochemical modeling. *Biogeosciences* **2013**, *10*, 2525–2537.

(12) Eger, A.; Almond, P. C.; Condron, L. M. Phosphorus fertilization by active dust deposition in a super-humid, temperate environment—Soil phosphorus fractionation and accession processes. *Global Biogeochem. Cycles* **2013**, *27*, 108–118.

(13) Blum, J. D.; Klaue, A.; Nezat, C. A.; Driscoll, C. T.; Johnson, C. E.; Siccama, T. G.; Eagar, C.; Fahey, T. J.; Likens, G. E. Mycorrhizal weathering of apatite as an important calcium source in base-poor forest ecosystems. *Nature* **2002**, *417*, 729–731.

(14) Eijlsink, L.; Krom, M.; Herut, B. Speciation and burial flux of phosphorus in the surface sediments of the Eastern Mediterranean. *Am. J. Sci.* **2000**, *300*, 483–503.

(15) Nenes, A.; Krom, M.; Mihalopoulos, N.; Van Cappellen, P.; Shi, Z.; Bougiatioti, A.; Zarmpas, P.; Herut, B. Atmospheric acidification of mineral aerosols: A source of bioavailable phosphorus for the oceans. *Atmos. Chem. Phys.* **2011**, *11*, 6265–6272.

(16) Stockdale, A.; Krom, M. D.; Mortimer, R. J. G.; Benning, L. G.; Carslaw, K. S.; Herbert, R. J.; Shi, Z.; Myriokefalitakis, S.; Kanakidou, M.; Nenes, A. Understanding the nature of atmospheric acid processing of mineral dusts in supplying bioavailable phosphorus to the oceans. *Proc. Natl. Acad. Sci. U.S.A.* **2016**, *113*, 14639.

(17) Hudson-Edwards, K. A.; Bristow, C. S.; Cibin, G.; Mason, G.; Peacock, C. L. Solid-phase phosphorus speciation in Saharan Bodé Depression dusts and source sediments. *Chem. Geol.* **2014**, *384*, 16–26.

(18) Gross, A.; Goren, T.; Pio, C.; Cardoso, J.; Tirosh, O.; Todd, M. C.; Rosenfeld, D.; Weiner, T.; Custódio, D.; Angert, A. Variability in sources and concentrations of Saharan dust phosphorus over the Atlantic Ocean. *Environ. Sci. Technol. Lett.* **2015**, *2*, 31–37.

(19) Longo, A. F.; Ingall, E. D.; Diaz, J. M.; Oakes, M.; King, L. E.; Nenes, A.; Mihalopoulos, N.; Violaki, K.; Avila, A.; Benitez-Nelson, C. R.; Brandes, J.; McNulty, I.; Vine, D. J. P-NEXFS analysis of aerosol phosphorus delivered to the Mediterranean Sea. *Geophys. Res. Lett.* **2014**, *41*, 4043–4049.

(20) Prospero, J. M.; Bonatti, E.; Schubert, C.; Carlson, T. N. Dust in the Caribbean atmosphere traced to an African dust storm. *Earth Planet. Sci. Lett.* **1970**, *9*, 287–293.

(21) Prospero, J. M.; Collard, F.-X.; Molinié, J.; Jeannot, A. Characterizing the annual cycle of African dust transport to the Caribbean Basin and South America and its impact on the environment and air quality. *Global Biogeochem. Cycles* **2014**, *28*, 757–773.

(22) Baker, A. R.; French, M.; Linge, K. L. Trends in aerosol nutrient solubility along a west–east transect of the Saharan dust plume. *Geophys. Res. Lett.* **2006**, *33*, No. L07805.

(23) Korte, L. F.; Pausch, F.; Trimborn, S.; Brussaard, C. P. D.; Brummer, G. J. A.; van der Does, M.; Guerreiro, C. V.; Schreuder, L. T.; Munday, C. I.; Stuut, J. B. W. Effects of dry and wet Saharan dust deposition in the tropical North Atlantic Ocean. *Biogeosci. Discuss.* **2018**, *2018*, 1–20.

(24) Olsson, P. Q.; Benner, R. L. Atmospheric Chemistry and Physics: From Air Pollution to Climate Change. *J. Am. Chem. Soc.* **1999**, *121*, 1423.

(25) Shi, Z.; Krom, M.; Bonneville, S. C.; Baker, A.; Jickells, T.; Benning, L. Formation of Iron Nanoparticles and Increase in Iron Reactivity in Mineral Dust during Simulated Cloud Processing. *Environ. Sci. Technol.* **2009**, *43*, 6592–6596.

(26) Shi, Z.; Krom, M. D.; Bonneville, S.; Baker, A. R.; Bristow, C.; Drake, N.; Mann, G.; Carslaw, K.; McQuaid, J. B.; Jickells, T.; Benning, L. G. Influence of chemical weathering and aging of iron oxides on the potential iron solubility of Saharan dust during simulated atmospheric processing. *Global Biogeochem. Cycles* **2011**, *25*, No. GB2010.

(27) Shi, Z.; Krom, M. D.; Bonneville, S.; Benning, L. G. Atmospheric Processing Outside Clouds Increases Soluble Iron in Mineral Dust. *Environ. Sci. Technol.* **2015**, *49*, 1472–1477.

(28) Longo, A. F.; Feng, Y.; Lai, B.; Landing, W. M.; Shelley, R. U.; Nenes, A.; Mihalopoulos, N.; Violaki, K.; Ingall, E. D. Influence of Atmospheric Processes on the Solubility and Composition of Iron in Saharan Dust. *Environ. Sci. Technol.* **2016**, *50*, 6912–6920.

(29) Denjean, C.; Caquineau, S.; Desboeufs, K.; Laurent, B.; Maille, M.; Quiñones Rosado, M.; Vallejo, P.; Mayol-Bracero, O. L.; Formenti, P. Long-range transport across the Atlantic in summertime does not enhance the hygroscopicity of African mineral dust. *Geophys. Res. Lett.* **2015**, *42*, 7835–7843.

(30) Maters, E.; Delmelle, P.; Bonneville, S. C. Atmospheric Processing of Volcanic Glass: Effects on Iron Solubility and Redox Speciation. *Environ. Sci. Technol.* **2016**, *50*, 5033–5040.

(31) Zhang, Z.; Goldstein, H. L.; Reynolds, R. L.; Hu, Y.; Wang, X.; Zhu, M. Phosphorus speciation and solubility in aeolian dust deposited in the interior American West. *Environ. Sci. Technol.* **2018**, *52*, 2658–2667.

(32) van der Does, M.; Korte, L. F.; Munday, C. I.; Brummer, G. J. A.; Stuut, J. B. W. Particle size traces modern Saharan dust transport and deposition across the equatorial North Atlantic. *Atmos. Chem. Phys.* **2016**, *16*, 13697–13710.

(33) Prospero, J. M. Long-range transport of mineral dust in the global atmosphere: Impact of African dust on the environment of the southeastern United States. *Proc. Natl. Acad. Sci. U.S.A.* **1999**, *96*, 3396.

(34) Liu, J.; Yang, J.; Liang, X.; Zhao, Y.; Cade-Menun, B. J.; Hu, Y. Molecular Speciation of Phosphorus Present in Readily Dispersible Colloids from Agricultural Soils. *Soil. Sci. Soc. Am. J.* **2014**, *78*, 47–53.

(35) Gross, A.; Turner, B.; Goren, T.; Berry, A.; Angert, A. Tracing the Sources of Atmospheric Phosphorus Deposition to a Tropical Rain Forest in Panama Using Stable Oxygen Isotopes. *Environ. Sci. Technol.* **2015**, *50*, 1147–1156.

(36) Stewart, J.; O'Halloran, I.; Kachanowski, R. Influence of texture and management practices on the forms and distribution of soil phosphorus. *Can. J. Soil Sci.* **1987**, *67*, 147–163.

(37) Kanakidou, M.; Myriokefalitakis, S.; Tsigaridis, K. Aerosols in atmospheric chemistry and biogeochemical cycles of nutrients. *Environ. Res. Lett.* **2018**, *13*, No. 063004.

(38) Barkley, A. E.; Prospero, J. M.; Mahowald, N.; Hamilton, D. S.; Popendorf, K. J.; Oehlert, A. M.; Pourmand, A.; Gatineau, A.; Panachou-Pulcherie, K.; Blackwelder, P.; Gaston, C. J. African biomass burning is a substantial source of phosphorus deposition to the Amazon, Tropical Atlantic Ocean, and Southern Ocean. *Proc. Natl. Acad. Sci. U.S.A.* **2019**, *116*, 16216.

(39) Laura, B.; Mayol-Bracero, O. L.; Santos, G.; Fishman, A.; Angert, A. Are the phosphate oxygen isotopes of Saharan dust a robust tracer of atmospheric P source? *Atmos. Environ.* **2020**, *235*, No. 117561.

(40) Prospero, J. M.; Glaccum, R. A.; Nees, R. T. Atmospheric transport of soil dust from Africa to South America. *Nature* **1981**, *289*, 570–572.

(41) Scheuvens, D.; Schütz, L.; Kandler, K.; Ebert, M.; Weinbruch, S. Bulk composition of northern African dust and its source sediments — A compilation. *Earth-Sci. Rev.* **2013**, *116*, 170–194.

(42) Gee, G. W.; Bauder, J. W. Particle-Size Analysis. In *Methods of Soil Analysis. Part 1. Physical and Mineralogical Methods*; American Society of Agronomy: Madison, WI, 1986.

(43) Murphy, J.; Riley, J. P. A modified single solution method for the determination of phosphate in natural waters. *Anal. Chim. Acta* **1962**, *27*, 31–36.

(44) Prietzel, J.; Dümg, A.; Wu, Y.; Zhou, J.; Klysubun, W. Synchrotron-based P K-edge XANES spectroscopy reveals rapid changes of phosphorus speciation in the topsoil of two glacier foreland chronosequences. *Geochim. Cosmochim. Acta* **2013**, *108*, 154–171.

(45) Gu, C.; Hart, S. C.; Turner, B. L.; Hu, Y.; Meng, Y.; Zhu, M. Aeolian dust deposition and the perturbation of phosphorus transformations during long-term ecosystem development in a cool, semi-arid environment. *Geochim. Cosmochim. Acta* **2019**, *246*, 498–514.

(46) Aspila, K. I.; Agemian, H.; Chau, A. S. Y. A semi-automated method for the determination of inorganic, organic and total phosphate in sediments. *Analyst* **1976**, *101*, 187–197.

(47) Formenti, P.; Caquineau, S.; Desboeufs, K.; Klaver, A.; Chevallier, S.; Journet, E.; Rajot, J. L. Mapping the physico-chemical properties of mineral dust in western Africa: mineralogical composition. *Atmos. Chem. Phys.* **2014**, *14*, 10663–10686.

(48) Wise, M. E.; Semeniuk, T. A.; Bruintjes, R.; Martin, S. T.; Russell, L. M.; Buseck, P. R. Hygroscopic behavior of NaCl-bearing natural aerosol particles using environmental transmission electron microscopy. *J. Geophys. Res.* **2007**, *112*, No. D10224.

(49) Fitzgerald, E.; Ault, A. P.; Zauscher, M. D.; Mayol-Bracero, O. L.; Prather, K. A. Comparison of the mixing state of long-range transported Asian and African mineral dust. *Atmos. Environ.* **2015**, *115*, 19–25.

(50) Glaccum, R. A.; Prospero, J. M. Saharan aerosols over the tropical North Atlantic — Mineralogy. *Mar. Geol.* **1980**, *37*, 295–321.

(51) Korte, L. F.; Brummer, G. J. A.; van der Does, M.; Guerreiro, C. V.; Hennekam, R.; van Hateren, J. A.; Jong, D.; Munday, C. I.; Schouten, S.; Stuut, J. B. W. Downward particle fluxes of biogenic matter and Saharan dust across the equatorial North Atlantic. *Atmos. Chem. Phys.* **2017**, *17*, 6023–6040.

(52) van der Does, M.; Korte, L.; Munday, C.; Brummer, G.-J.; Stuut, J.-B. Particle size traces modern Saharan dust transport and deposition across the equatorial North Atlantic. *Atmos. Chem. Phys.* **2016**, *16*, 13697–13710.

(53) Formenti, P.; Schütz, L.; Balkanski, Y.; Desboeufs, K.; Ebert, M.; Kandler, K.; Petzold, A.; Scheuvens, D.; Weinbruch, S.; Zhang, D. Recent progress in understanding physical and chemical properties of African and Asian mineral dust. *Atmos. Chem. Phys.* **2011**, *11*, 8231–8256.

(54) Yu, Y.; Kalashnikova, O. V.; Garay, M. J.; Lee, H.; Notaro, M.; Campbell, J. R.; Marquis, J.; Ginoux, P.; Okin, G. S. Disproving the Bodélé Depression as the Primary Source of Dust Fertilizing the Amazon Rainforest. *Geophys. Res. Lett.* **2020**, *47*, No. e2020GL088020.

(55) Koren, I.; J Kaufman, Y.; Washington, R.; Todd, M.; Rudich, Y.; Vanderlei Martins, J.; Rosenfeld, D. The Bodélé depression: A single spot in the Sahara that provides most of the mineral dust to the Amazon Forest. *Environ. Res. Lett.* **2006**, *1*, No. 014005.

(56) Bristow, C. S.; Hudson-Edwards, K. A.; Chappell, A. Fertilizing the Amazon and equatorial Atlantic with West African dust. *Geophys. Res. Lett.* **2010**, *37*, No. L14807.

(57) O'Day, P. A.; Nwosu, U. G.; Barnes, M. E.; Hart, S. C.; Berhe, A. A.; Christensen, J. N.; Williams, K. H. Phosphorus Speciation in Atmospherically Deposited Particulate Matter and Implications for Terrestrial Ecosystem Productivity. *Environ. Sci. Technol.* **2020**, *54*, 4984–4994.

(58) Prospero, J. M.; Ginoux, P.; Torres, O.; Nicholson, S. E.; Gill, T. E. Environmental characterization of global sources of atmospheric soil dust identified with the NIMBUS 7 Total Ozone Mapping Spectrometer (TOMS) absorbing aerosol product. *Rev. Geophys.* **2002**, *40*, 2–1–2–31.

(59) Kumar, A.; Abouchami, W.; Galer, S. J. G.; Singh, S. P.; Fomba, K. W.; Prospero, J. M.; Andreae, M. O. Seasonal radiogenic isotopic variability of the African dust outflow to the tropical Atlantic Ocean and across to the Caribbean. *Earth Planet. Sci. Lett.* **2018**, *487*, 94–105.

(60) Pourmand, A.; Prospero, J. M.; Sharifi, A. Geochemical fingerprinting of trans-Atlantic African dust based on radiogenic Sr-Nd-Hf isotopes and rare earth element anomalies. *Geology* **2014**, *42*, 675–678.

(61) van der Does, M.; Pourmand, A.; Sharifi, A.; Stuut, J.-B. W. North African mineral dust across the tropical Atlantic Ocean: Insights from dust particle size, radiogenic Sr-Nd-Hf isotopes and rare earth elements (REE). *Aeolian Res.* **2018**, *33*, 106–116.

(62) Heartsill-Scalley, T.; Scatena, F. N.; Estrada, C.; McDowell, W. H.; Lugo, A. E. Disturbance and long-term patterns of rainfall and throughfall nutrient fluxes in a subtropical wet forest in Puerto Rico. *J. Hydrol.* **2007**, *333*, 472–485.

(63) F Graham, W.; Duce, R. Atmospheric Input of Phosphorus to Remote Tropical Islands. *Pac. Sci.* **1981**, *35*, 241–255.

(64) Quijano, L.; Kuhn, N. J.; Navas, A. Effects of interrill erosion on the distribution of soil organic and inorganic carbon in different sized particles of Mediterranean Calcisols. *Soil Tillage Res.* **2020**, *196*, No. 104461.

(65) Wang, X.; Hu, Y.; Tang, Y.; Yang, P.; Feng, X.; Xu, W.; Zhu, M. Phosphate and phytate adsorption and precipitation on ferrhydrite surfaces. *Environ. Sci. Nano* **2017**, *4*, 2193–2204.

(66) Wang, X.; Phillips, B. L.; Boily, J.-F.; Hu, Y.; Hu, Z.; Yang, P.; Feng, X.; Xu, W.; Zhu, M. Phosphate Sorption Speciation and Precipitation Mechanisms on Amorphous Aluminum Hydroxide. *Soil Syst.* **2019**, *3*, No. 20.

(67) Herut, B.; Krom, M. D.; Pan, G.; Mortimer, R. Atmospheric input of nitrogen and phosphorus to the Southeast Mediterranean:

Sources, fluxes, and possible impact. *Limnol. Oceanogr.* **1999**, *44*, 1683–1692.

(68) Schachtman, D. P.; Reid, R. J.; Ayling, S. M. Phosphorus Uptake by Plants: From Soil to Cell. *Plant Physiol.* **1998**, *116*, 447.

(69) Negreiros, G. H. d.; Nepstad, D. C. In *Mapping Deeply Rooting Forests of Brazilian Amazonia with GIS*, Proceedings of ISPRS Commission VII Symposium; Resource and Environmental Monitoring: Rio de Janeiro, 1994; pp 334–338.

(70) Zhang, Z.; Zhao, Z.; Liu, C.; Chadwick, O. A.; Liang, C.; Hu, Y.; Vaughan, K. L.; Zhu, M. Vertical patterns of phosphorus concentration and speciation in three forest soil profiles of contrasting climate. *Geochim. Cosmochim. Acta* **2021**, *310*, 1–18.

(71) Vogel, C.; Helfenstein, J.; Massey, M. S.; Sekine, R.; Kretzschmar, R.; Beiping, L.; Peter, T.; Chadwick, O. A.; Tamburini, F.; Rivard, C.; Herzl, H.; Adam, C.; Pradas del Real, A. E.; Castillo-Michel, H.; Zuin, L.; Wang, D.; Félix, R.; Lassalle-Kaiser, B.; Frossard, E. Microspectroscopy reveals dust-derived apatite grains in acidic, highly-weathered Hawaiian soils. *Geoderma* **2021**, *381*, No. 114681.